Contents lists available at ScienceDirect

Computational Materials Science

journal homepage: www.elsevier.com

# The effect of introducing stochasticity to kinetic mean-field calculations: Comparison with lattice kinetic Monte Carlo in case of regular solid solutions

Tetyana V. Zaporozhets [a], Andriy Taranovskyy [b], Gabriella Jáger [b], Andriy M. Gusak [a], Zoltán Erdélyi [b], János J. Tomán [b,*]

[a] Department of Physics, Cherkasy National University, Shevchenko Street 81, Cherkasy 18031, Ukraine
[b] Department of Solid State Physics, University of Debrecen, P.O. Box 400, H-4002 Debrecen, Hungary

ARTICLE INFO

*Keywords:*
Regular solution
Mean-field
Monte Carlo
Thermodynamics of solutions
Noise
Fluctuation phenomena
Statistical mechanics of model systems

ABSTRACT

In present work we discuss the problem of introducing stochasticity into 3D atomistic kinetic mean-field simulations. As this is a new approach for simulating the time evolution of material systems, it should be positioned in the field of available methods. Compared to the most used stochastic techniques: while atomistic kinetic Monte Carlo (KMC) methods generate microstates of the system they simulate, stochastic kinetic mean-field (SKMF) seems to generate mesostates of the system during a finite time-window. Previously, strong interrelation have been found for the dispersion of composition fluctuations in ideal solutions between SKMF states and averaged KMC states. In present work we compare the statistical nature of fluctuations in the two approaches in case of equilibrium solid solutions with non-zero mixing energies. At the investigated high temperature cases we show how at a certain noise amplitude in SKMF the composition fluctuations can be related to results received by averaging a certain number of independent KMC states. Furthermore, the correlation between the neighboring sites, emerging because of the chemical interactions, shows the same statistical behavior in both methods as well.

## 1. Introduction

Mean-field approach is a well-known "zero-approximation" approach to many physical and chemical problems enabling to grasp the basic characteristic of many phenomena without pretending on rigorous derivations and results. Among the most popular examples-Van der Waals theory of real gas [1], Vlasov kinetic mean-field equation for many-body systems and its application to plasma as well as to so-called "non-local crystal theory" [2,3], Weiss mean-field model of magnetism [4], Hartree-Fock self consistent (mean-field) approach to electron configurations in atoms and crystals [5], Bragg-Williams approximation in ordering theory [6], Khachaturyan's concentration waves approach to the theory of alloys [7]. An interesting quasi-1D modification of the mean-field approach to kinetic problems of atomic transport in solid state was suggested by George Martin in 1990 [8]. Martin's scheme (Kinetic Mean-Field – KMF) self-consistently reproduces Boltzmann distribution in the marginal equilibrium case. Application of this scheme to the initial stages of interdiffusion in nanofilms with a strong diffusion asymmetry demonstrated the possibility of sharpening of diffusion profile instead of broadening. This predicted effect was found experimentally [9,10]. It was also used for calculating kinetics and size effects in surface segregation phenomena [11,12].

In Martin's kinetic mean-field model the temperature effect is taken into account via Arrhenius law for jump frequencies and for corresponding atomic fluxes. Yet, since the concept is a mean-field one, the fluctuations in free energy, in this model, can only relax but never be created! [13] "In real life", homo-phase and hetero-phase fluctuations are also related to temperature, but in the mean-field model this side of it is not considered. Thus, the account of temperature in the mean-field concept is not complete. It takes into account the overcoming of barriers during atomic jumps, but not the overcoming of nucleation barriers, due to neglect of concentration and order fluctuations. Thus, the first-order transitions cannot be properly described.

To compensate this drawback, noise can be introduced into the mean-field scheme. In case of atomic transport, the noise of concentration and of order parameter was introduced into the Onsager scheme following the fluctuation–dissipation theorem, for example, by Khachaturyan et al. [14,15]. Yet, this method had some limitations: (i) Onsager scheme for atomic local fluxes was linear and not self-

* Corresponding author.
*Email address:* janos.toman@science.unideb.hu (J.J. Tomán)

https://doi.org/10.1016/j.commatsci.2019.109251
Received 3 March 2019; Received in revised form 30 July 2019; Accepted 28 August 2019
Available online xxx
0927-0256/ 

consistent: Onsager coefficients and their activation energies were not interrelated with local composition and its energetics (contrary to Martin's approach). In reality, during the very initial stages of diffusion in highly asymmetric systems the flux is not proportional to the difference of chemical potentials, but, for example, to the difference of their exponents [16,17], (ii) Order parameter fluctuations were introduced independently of concentration fluctuation. On the contrary, in Martin's approach the order is not something independent, instead it is determined by the oscillations of local concentration (unary probabilities at the sites) between sublattices.

Introduction of stochasticity into Martin's mean-field approach must be possible in many different ways. One is that instead of applying the noise directly as composition fluctuations, it is introduced into the system via the uncertainty of the atomic flux. There are at least two ways one can argue that this is physically viable: i) Even if jump frequency (inverse transition time) is fixed, the number of transitions during some finite time interval *dt* is a random value governed by Poisson distribution - and it provides the scattering of the atomic flux (number of transitions per *dt*) ii) In an alloy the activation energy of a jump depends on the exact atomic configuration. At the same mean composition we always have the spectrum of possible configurations, and hence, the spectrum of jump frequencies – in this case, the stochasticity arises in the jump frequency itself.

The stochastic kinetic mean-field approach is useful, because the resulting states of the system are close to what an imaginary, atomistic measurement would see during a finite time window. One might see it as a coarse-grained view of the timescale. This makes the processing and understanding of the results usually quite straightforward. Though, understanding exactly what is happening in an atomistic kinetic mean-field model if it is "stochasticised" via the microscopic fluxes is important for positioning its applicability. The results shown in present work are but one step of a long journey understanding the nature of fluctuations in SKMF. First, we will investigate the fluctuations of homogeneous, high-temperature states of binary systems with chemical interactions between the species, where both positive and negative mixing energies will be considered.

## 2. Theoretical background

In Martin's approach the master equation for $C_i$ finding probability of A atom on site *i*, based on balance of local in- and out- fluxes for any site, self-consistently used the mean-field approximation for calculation of energy barriers in the jump frequencies. In the case of exchange mechanism in 3D lattice with $Z$ sites in the first coordination shell it means [18]:

$$\frac{dC_i}{dt} = -\sum_{j=1}^{Z}\left[J_{i,j}^{\mathrm{MF}} - J_{j,i}^{\mathrm{MF}}\right] = -\sum_{j=1}^{Z}\left[\underbrace{C_i\left(1-C_j\right)\Gamma_{i,j}}_{J_{i,j}^{MF}} - \underbrace{\left(1-C_i\right)C_j\Gamma_{j,i}}_{J_{j,i}^{MF}}\right]. \quad (1)$$

The $\Gamma_{i,j}$ exchange frequencies between $A$ and $B$ on the neighboring sites $i$ and $j$, accordingly, are determined in [8,18] via Arrhenius law like

$$\Gamma_{i,j} = \nu_0 \exp\left(-\frac{Q_{i,j}}{\mathrm{k_B}T}\right) = \nu_0 \exp\left(-\frac{E^{\mathrm{saddle}} - \left(E_i^A + E_j^B\right)}{\mathrm{k_B}T}\right), \quad (2)$$

where $\mathrm{k_B}$ is the Boltzmann constant, $T$ is the absolute temperature, $\nu_0$ denotes the attempt frequency (related to the Debye-frequency), $E^{\mathrm{saddle}}$ is the saddle-point energy (here assumed to be the same for all jumps). $E_i^A$ and $E_j^B$ energies before jump are calculated in the nearest neighbor pair interactions approximation ($V_{AA}$,$V_{BB}$,$V_{AB}$) and without any account of correlations – in the mean-field approximation:

$$E_i^A = \sum_{in=1}^{Z}\left[C_{in}V_{AA} + \left(1-C_{in}\right)V_{AB}\right], E_j^B = \sum_{jn=1}^{Z}\left[C_{jn}V_{AB} + \left(1-C_{jn}\right)V_{BB}\right], \quad (3)$$

where *in* is the nearest neighbor of site *i* and *jn* is the nearest neighbor of site *j*. Separating all the composition independent parts we can introduce $\Gamma_0$:

$$\Gamma_{i,j} = \underbrace{\nu_0 \exp\left(-\frac{E^{\mathrm{saddle}} - Z\left(V_{AB}+V_{BB}\right)}{\mathrm{k_B}T}\right)}_{\Gamma_0} \exp\left(\frac{\hat{E}_{i,j}}{\mathrm{k_B}T}\right) = \Gamma_0 \exp\left(\frac{(M-V)\sum_{in=1}^{Z}C_{in} + (M+V)\sum_{jn=1}^{Z}C_{jn}}{\mathrm{k_B}T}\right), \quad (4)$$

where $V = V_{AB} - \left(V_{AA}+V_{BB}\right)/2$ is the energy of mixing and $M = \left(V_{AA}-V_{BB}\right)/2$ is the term that represents the exponentially composition dependent diffusion coefficient [19].

In 2016 we introduced a new simulation method called SKMF (Stochastic Kinetic Mean-Field), based on introduction of the noise in the reason of fluctuations of composition instead of directly fluctuating it [20]. This can be achieved by replacing $J_{i,j}^{\mathrm{MF}}$ and its pair $J_{j,i}^{\mathrm{MF}}$ in Eq. (1) with sums of two parts:

$$\frac{dC_i}{dt} = -\sum_{j=1}^{Z}\left[J_{i,j} - J_{j,i}\right], \quad (5)$$

$$J_{i,j} = J_{i,j}^{\mathrm{MF}} + \delta J_{i,j}^{\mathrm{Lang}} \quad \text{and} \quad J_{j,i} = J_{j,i}^{\mathrm{MF}} + \delta J_{j,i}^{\mathrm{Lang}}, \quad (6)$$

where $J_{i,j}^{\mathrm{MF}}$ and $J_{j,i}^{\mathrm{MF}}$ remain the same mean-field approximation for atomic fluxes, but they are extended by an additive dynamic Langevin noise term:

$$\delta J_{i,j}^{\mathrm{Lang}} = c_i\left(1-c_j\right)\frac{A_n}{\sqrt{dt}}\sqrt{3}\left(2u_1-1\right), \delta J_{j,i}^{\mathrm{Lang}} = c_j\left(1-c_i\right)\frac{A_n}{\sqrt{dt}}\sqrt{3}\left(2u_2-1\right), \quad (7)$$

where $A_n$ is the noise amplitude, *dt* is the simulation timestep and $u_1$ and $u_2$ are independent, uniform distribution random numbers on the [0,1) interval. For considerations on the detailed balance see Section II. of [21]. Alternatively, one can use many different noise implementations. An option can be noise with normal distribution generated by the Box-Muller transform [22] from two uniformly distributed random numbers on the [0,1) interval. Though, in our implementation we used (7) and the investigation of the effects of different noise implementations is beyond the scope of this work. We previously applied this type of noise for exchange mechanism and also for vacancy mechanism. It was utilized for modelling precipitation, spinodal decomposition, tracer diffusion, ordering, ternary systems etc. [23–26]. Nevertheless, so far the basic principles of SKMF approach were discussed and proved in details only for the case of ideal solution [20]. Namely, for the case of ideal

solution:

a)Composition deviation (mean squared fluctuation of composition at one site) is proportional to the squared noise amplitude:

$$\left\langle \left(\delta C_i\right)^2 \right\rangle = \left[ \frac{\overline{C_i}\left(1-\overline{C_i}\right)A_n}{\sqrt{\Gamma_0}} \right]^2. \tag{8}$$

b)Using of certain noise amplitude in SKMF is equivalent to averaging $\mathscr{M}$ runs of Monte Carlo simulations, with

$$\mathscr{M} = \frac{\Gamma_0}{\overline{C}\left(1-\overline{C}\right)A_n^2}. \tag{9}$$

In other words, $\mathscr{M}$ is a finite number of copies in the canonical ensemble over which the averaging is done. Zero noise is equivalent to the infinite number of copies in the canonical ensemble, and it is mean-field.

Both Eqs. (8) and (9) were discussed, proven analytically and checked numerically for the case of ideal solution in Ref. [20].

In present work we consider in details the fluctuations in non-ideal solutions with positive as well as with negative $V$ mixing energies (meaning tendency to phase separation and ordering, respectively). We will examine "high" temperature solutions, by which we mean:

$$\frac{k_B T}{|V|} > \frac{Z}{2}, \tag{10}$$

when the regular solution is beyond the critical temperature, so there is only one stable, solution phase in both immiscible ($V > 0$) and ordering systems ($V < 0$). In the modelled FCC systems ($Z = 12$) this will mean $|V| < 0.166\acute{6} k_B T$ values for every cases.

Here we will consider a homogeneous (apart from local fluctuations) binary FCC solid solution with equal average probability (concentration) of A atom being found at any site:

$$\langle C_i \rangle = \left\langle C_j \right\rangle = \overline{C}. \tag{11}$$

Local concentration (at site $i$) is fluctuating:

$$C_i = \overline{C} + \delta C_i. \tag{12}$$

As before, we are, first of all, interested in concentration dispersion (which is of course positive and the same for each site of globally homogeneous system:

$$x_0 \equiv \langle \delta C_i \delta C_i \rangle. \tag{13}$$

Composition fluctuation in clusters containing central atom and all or some part of the nearest neighborhood, can be found for various cluster definitions. In this work we use the following:

$$x_{0,\text{cluster}} = \left\langle \left( \frac{\delta C_i + \sum_{in=1}^{Z} \delta C_{in}}{1+Z} \right)^2 \right\rangle. \tag{14}$$

Here 1 represents the central atom and $Z = 12$ is the number of sites in the first coordination shell.

Despite initial neglect of correlation in the basic equations of SKMF, it is physically evident that in case of positive mixing energy, when the alloy has a tendency to decomposition (which becomes successful at low temperature), the neighboring sites should demonstrate the tendency to fluctuations of the same sign, so that the spatial correlation

$$x_1 \equiv \langle \delta C_i \delta C_{in} \rangle \tag{15}$$

is expected to be not zero, but positive. On the contrary, in case of negative mixing energy, when the alloy has a tendency to ordering, $x_1$ is expected to be not zero, but negative.

Immediate reason of correlations is a dependence of jump frequencies on the local concentration fluctuations:

$$\begin{aligned} \Gamma_{i,j} = & \quad \nu_0 \exp\left(-\frac{Q_{i,j}}{k_B T}\right) = \\ = & \quad \nu_0 \exp\left(-\frac{E^{\text{saddle}} - \left(E_i^A + E_j^B\right)}{k_B T}\right) = \\ = & \quad \underbrace{\nu_0 \exp\left(-\frac{E^{\text{saddle}} - \left(\overline{E^A} + \overline{E^B}\right)}{k_B T}\right)}_{\bar{\Gamma}} \exp\left(\frac{\delta E_i^A + \delta E_j^B}{k_B T}\right) \approx \\ \approx & \quad \bar{\Gamma}\left(1 + \frac{\delta E_i^A + \delta E_j^B}{k_B T}\right). \end{aligned} \tag{16}$$

It is easy to show that

$$\begin{aligned} \overline{E}_A + \overline{E}_B &= Z\left(\overline{C}V_{AA} + \left(1-\overline{C}\right)V_{AB}\right) + \\ &+ Z\left(\overline{C}V_{AB} + \left(1-\overline{C}\right)V_{BB}\right) = \\ &= Z\left(V_{AB} + V_{BB}\right) + Z\left(V_{AA} - V_{BB}\right)\overline{C}. \end{aligned} \tag{17}$$

Therefore,

$$\begin{aligned} \bar{\Gamma} = & \quad \nu_0 \exp\left(-\frac{E^{\text{saddle}} - Z(V_{AB}+V_{BB})}{k_B T}\right) \exp\left(\frac{2ZM\overline{C}}{k_B T}\right) \equiv \\ \equiv & \quad \Gamma_0 \exp\left(m\overline{C}\right), \end{aligned} \tag{18}$$

where $M = \left(V_{AA} - V_{BB}\right)/2$ and using the notation of Ref. [19]

$$m = 2Z\frac{M}{k_B T} \tag{19}$$

for the exponential composition dependence of interdiffusion coefficient:

$$D(C) = D_0 \exp(mC). \tag{20}$$

## 3. Method of comparing SKMF to atomistic lattice kinetic Monte Carlo simulations

To gather the statistical data from SKMF simulations we used a sample with $(20 \times 20 \times 20)/2$ sites with periodic boundary conditions. The simulations were run using dimensionless parameters, $\widetilde{V} \equiv V/\left(k_B T\right)$ and $\widetilde{A}_n \equiv A_n/\sqrt{\Gamma_0}$ and the dimensionless timestep was $d\tau \equiv dt \cdot \Gamma_0 = 10^{-3}$ and were started from homogeneous $\overline{C}$ composition. The system was left for $10^4$ timesteps to thermalize, afterwards the statistics were collected over $10^5$ timesteps. The results did not change significantly by either increasing the system size or the averaging time interval or by changing the timestep.

In Ref. [20] comparison of SKMF composition fluctuations to the ones in averaged runs of one-vacancy residence time atomistic kinetic Monte Carlo (KMC) was made. It is important to note that because we average independent states, in this comparison the exact method behind kinetic Monte Carlo is not important. It is just a way to generate independent microstates of the system. Furthermore, the mean squared fluctuation of composition is determined only by the thermodynamics [27]. In present work we do not investigate the kinetics, where the correlation effects of the vacancy mechanism would be important in KMC. In the applied averaging scheme it has no effect at all. The interaction energies between atoms and the vacancy are $V_{AV} = V_{BV} = 0$, otherwise the same thermodynamic parameters were used.

We follow up with the idea and in this work we perform the comparison for regular solid solutions. For this we extended out the

way we average the states of KMC simulations. In [20] KMC runs were started from the same random configuration and separate runs have been averaged after 80 Monte Carlo steps (MCS). (By 1 MCS we understand the number of vacancy jumps where *on average* every atom of the system jumped once, i.e. for a system with 4000 sites this means 4000 vacancy jumps.) In current work we changed the method slightly and for this we applied the ergodicity idea (average over ensemble for the system in equilibrium is equal to the average over time). During the Monte Carlo simulation starting from a random configuration in a system containing $(20\times20\times20)/2$ particles (of which one was a vacany) with periodic boundary conditions we saved the states of the system after every 100 MCS. In these regular solid solutions the saved states can be considered as completely independent, though, still part of the same timeline. (Let us note that while in this work this might not play a huge role, in other cases this approach might make the comparison of SKMF and KMC possible not only in the case of equilibrium states or during steady-state processes. It is very likely, that in non-equilibrium or non-steady-state cases the averaging technique for KMC should be more sofisticated, e.g. using exponentially weighted moving average [28,29], and that will probably modify the relationship between the two methods. Even though the authors have the intent to investigate such scenarios in the future, it is beyond the scope of current work.) Then we averaged $\mathscr{M}$ number of states as a moving average using the compositions (0,1 or 0.5 for the vacany) on the same site in the different states following each-other by 100 MCS. Then we used these average compositions as finding probabilities and similarly to SKMF we calculated composition dispersion $x_0$ and spatial correlation $x_1$.

## 4. Results and discussion

The rather complex, but still approximation-heavy theoretical reasoning behind the results can be found in the Supplementary Materials [30] and in [13]. The analytical calculations generally show the same tendency as the simulations and for $\widetilde{V}$ values not too far from 0 give very good approximations of the simulation results. Note, that in the followings we take the case of $\overline{C}=0.5$ and $M=0$ for which $\overline{\Gamma}=\Gamma_0$:

$$\widetilde{A}_n^{*} \equiv \frac{A_n}{\sqrt{\overline{\Gamma}}} = \frac{A_n}{\sqrt{\Gamma_0}} = \widetilde{A}_n. \tag{21}$$

The main idea of the previous results obtained in paper [20] can be demonstrated again by Fig. 1. using now the new averaging method, in which results of SKMF calculations and averaged KMC calculations are superimposed.

The logarithm of $x_0^{\mathrm{SKMF}}$ dispersion in SKMF is plotted against the logarithm of $\widetilde{A}_n^2$ squared noise amplitude (bottom $x$ axis), and simultaneously the logarithm of $x_0^{\mathrm{KMC}}$ dispersion in KMC (averaged over $\mathscr{M}$ Monte Carlo states, in other words, over $\mathscr{M}$ copies of the ensemble) is plotted against the logarithm of $\mathscr{M}^{-1}$ (top $x$ axis). Not only the slopes (equalling 1) coincide, but even the values. This means full mutual correspondence in ideal solutions between Monte Carlo averaged over $\mathscr{M}$ copies and SKMF disturbed by noise of flux with squared amplitude $\widetilde{A}_n^2 = 1/\left[\overline{C}\left(1-\overline{C}\right)\mathscr{M}\right]$.

When, in this paper, we switch to non-ideal solid solutions with non-zero mixing energies, the proportionality still holds, but the constants of proportionality $k_{0,\mathrm{site}}$ in the following equations become a function of $\widetilde{V}$ [13]:

$$x_0^{\mathrm{SKMF}} = k_{0,\mathrm{site}}^{\mathrm{SKMF}} \times \left[\overline{C}\left(1-\overline{C}\right)\widetilde{A}_n\right]^2, \tag{22}$$

$$x_0^{\mathrm{KMC}} = k_{0,\mathrm{site}}^{\mathrm{KMC}} \times \left[\overline{C}\left(1-\overline{C}\right)\mathscr{M}^{-1}\right]. \tag{23}$$

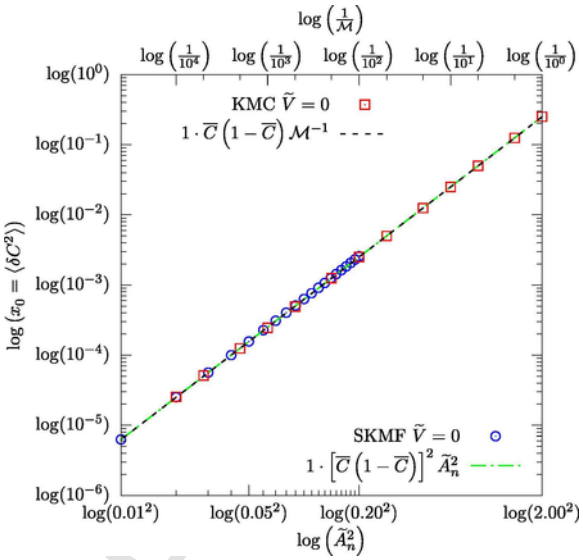


**Fig. 1.** Proportonality of $x_0$ in ideal solid solution with $\widetilde{A}_n^2$ in SKMF simulations (bottom $x$-axis) and with $\mathscr{M}^{-1}$ in averaged KMC simulations (top $x$-axis). Note, that the straight lines are not fits, but the analytical predictions from Eqs. (8) and (9).

Note, that on the double-logarithmic scale of Fig. 1 the change in $k_{0,\mathrm{site}}$ would result in a vertical shift with a slope still equalling to 1. Independently performing the fittings for SKMF and KMC results in cases of different $\widetilde{V}$ values, then plotting the $k_{0,\mathrm{site}}\left(\widetilde{V}\right)$ functions, we receive the data shown in Fig. 2. The SKMF results resemble very much the theoretically estimated curve [30]. But as we are averaging independent states of the KMC simulations, our finding probabilities received by the averaging process are simply statistical values, consequently independent of $\widetilde{V}$. Though, the high value at $\widetilde{V}=0.16$ raises the possibility that in that case the sampling distance of 100 MCS was not high enough. Furthermore, this might point to the direction, how introducing a different averaging scheme to KMC might keep the time correlation and would result in a similar behavior to SKMF, but the authors will keep the testing of this idea for another time.

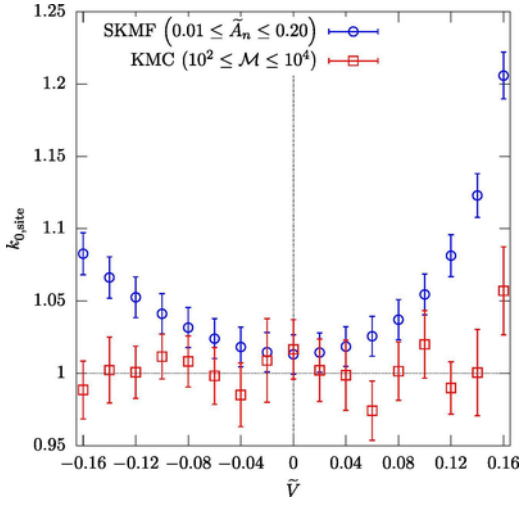


**Fig. 2.** Fitted $k_{0,\mathrm{site}}$ values of Eqs. (22) and (23). For SKMF we used results from 20 different noise amplitudes between 0.01 and 0.20 for the fitting. For KMC we used 7 different $\mathscr{M}$ values between $10^2$ and $10^4$, which covers roughly the same range in $x_0$. (See Fig. 1.) The error bars shown are the uncertainty of the fitted $k_{0,\mathrm{site}}$ values [31] and represent $\pm 2\sigma$, e.g. the 95% confidence levels. The relative standard deviation of the sampled $x_0$ values were always under 3.5%.

If we really want to compare the dispersion in the two different simulation techniques for regular solutions without complicating the averaging process of KMC, we should use a cluster containing more than one site. In the current work we used a cluster of 13 atoms (1 center atom with its 12 nearest neighbors) described by Eq. (14). Fitting $k_{0,\mathrm{cluster}}$ constants of proportionality in [30,13]:

$$x_{0,\mathrm{cluster}}^{\mathrm{SKMF}} = k_{0,\mathrm{cluster}}^{\mathrm{SKMF}} \times \left[\overline{C}\left(1-\overline{C}\right)\widetilde{A}_n\right]^2, \tag{24}$$

$$x_{0,\mathrm{cluster}}^{\mathrm{KMC}} = k_{0,\mathrm{cluster}}^{\mathrm{KMC}} \times \left[\overline{C}\left(1-\overline{C}\right)\mathscr{M}^{-1}\right], \tag{25}$$

for SKMF and KMC independently for different values of $\widetilde{V}$, the dependence on it is shown in Fig. 3. Comparing SKMF and KMC results, the similar behavior is evident by the figure (that also resembles the theoretically estimated behavior [30]), but larger and larger deviation can be seen the further away $\widetilde{V}$ gets from 0.

Looking at the definition in Eq. (14) it is clear that the site-wise dispersion affects the cluster-wise dispersion, so some normalization can be done. Note, that because both $x_{0,\mathrm{cluster}}$ and $x_0$ are proportional to $\widetilde{A}_n^2$ squared noise amplitude in SKMF and to $\mathscr{M}^{-1}$ reciprocal averaged number of states in KMC:

$$\text{in SKMF}: \quad \frac{x_{0,\mathrm{cluster}}^{\mathrm{SKMF}}}{x_0^{\mathrm{SKMF}}} = \frac{k_{0,\mathrm{cluster}}^{\mathrm{SKMF}} \times \left[\overline{C}\left(1-\overline{C}\right)\widetilde{A}_n\right]^2}{k_{0,\mathrm{site}}^{\mathrm{SKMF}} \times \left[\overline{C}\left(1-\overline{C}\right)\widetilde{A}_n\right]^2} = \frac{k_{0,\mathrm{cluster}}^{\mathrm{SKMF}}}{k_{0,\mathrm{site}}^{\mathrm{SKMF}}} \tag{26}$$

$$\text{in KMC}: \quad \frac{x_{0,\mathrm{cluster}}^{\mathrm{KMC}}}{x_0^{\mathrm{KMC}}} = \frac{k_{0,\mathrm{cluster}}^{\mathrm{KMC}} \times \left[\overline{C}\left(1-\overline{C}\right)\mathscr{M}^{-1}\right]}{k_{0,\mathrm{site}}^{\mathrm{KMC}} \times \left[\overline{C}\left(1-\overline{C}\right)\mathscr{M}^{-1}\right]} = \frac{k_{0,\mathrm{cluster}}^{\mathrm{KMC}}}{k_{0,\mathrm{site}}^{\mathrm{KMC}}} \tag{27}$$

$x_{0,\mathrm{cluster}}/x_0 = k_{0,\mathrm{cluster}}/k_{0,\mathrm{site}}$ is a measure, which is independent of $\widetilde{A}_n^2$ noise amplitude in SKMF and also independent of $\mathscr{M}^{-1}$ reciprocal averaged number of states in KMC. Consequently, $k_{0,\mathrm{cluster}}/k_{0,\mathrm{site}}$ should depend only on the thermodynamics of the system. This is exactly what we can see in Fig. 4., the points from SKMF and KMC match perfectly, proving the mutual correspondence between the two methods in case of regular solid solutions, too.

It can be shown that in regular solutions spatial correlation between neighboring atoms emerges. (For details see the Supplementary Materials [30].) When comparing the two simulation techniques, we must investigate if their behavior is similar in this sense, too. In Fig. 5. we show the dependence of $x_1 \equiv \langle \delta C_i \delta C_{in} \rangle$ on $\widetilde{V}$ in two-two cases for both SKMF and KMC. The particular values of $\widetilde{A}_n^2$ and $\mathscr{M}$ were chosen for visualization purposes based on similar $x_0$ dispersion values in the case of $\widetilde{V}=0$. (See Fig. 1.) Comparing the results of SKMF and KMC simulations, the behavior is similar to previous ones, the deviation of the two methods seemingly gets larger with the larger absolute value of $\widetilde{V}$. In Fig. 6. we show the dependence of $x_1$ on $\widetilde{A}_n^2$ in SKMF (bottom *x*-axis) and on $\mathscr{M}^{-1}$ in KMC (top *x*-axis) for two values of $\widetilde{V}$. The slopes of the fitted lines are 1 due to the double-logarithmic plotting and the proportionality between $x_1^{\mathrm{SKMF}}$ and $\widetilde{A}_n^2$ squared noise amplitude in SKMF (bottom *x*-axis) and between $x_1^{\mathrm{KMC}}$ and $\mathscr{M}^{-1}$ inversed number of averaged states in KMC (top *x-axis)*.

Once again, in regular solutions the $k_1$ constant of proportionality depends on $\widetilde{V}$ in the following equations [30,13]

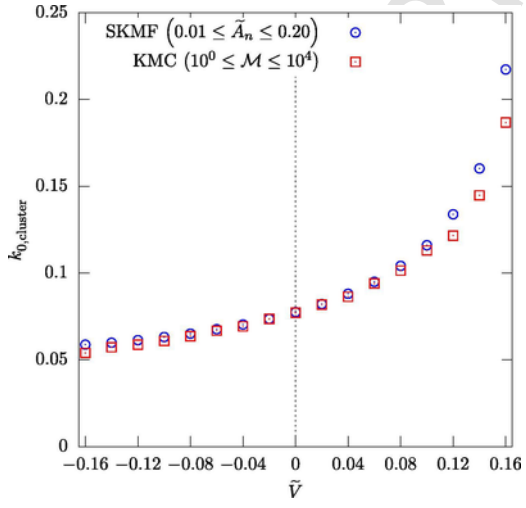


**Fig. 3.** Dependence of fitted proportionality factor $k_{0,\mathrm{cluster}}$ on $\widetilde{V}$ in Eqs. (24) and (25). The relative asymptotic standard error of fitting $k_{0,\mathrm{cluster}}$ to the average $x_{0,\mathrm{cluster}}$ values remained under 0.5% for all cases of SKMF and under 2.5% for all cases of KMC. Error bars are not shown for the sake of clarity as they would be similar in size to the markers used.

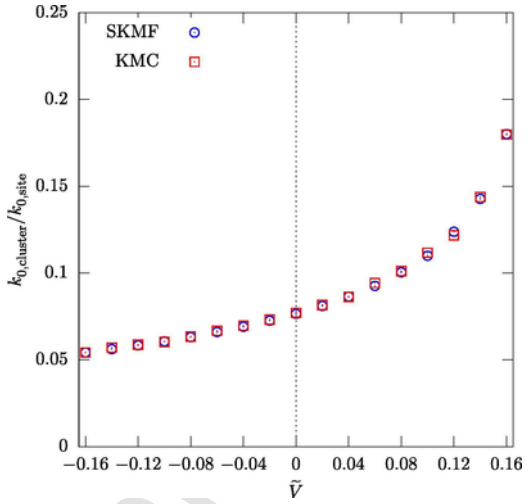


**Fig. 4.** Fitted constants of proportionality $k_{0,\mathrm{cluster}}$ from Eqs. (24) and (25) (See Fig. 3.) divided by the according fitted constants of proportionality $k_{0,\mathrm{site}}$ from Eqs. (22) and (23) (See Fig. 2.). At a certain $\overline{C}$ average composition $k_{0,\mathrm{cluster}}/k_{0,\mathrm{site}}$ depends only on the thermodynamic parameters of the system and accordingly, SKMF and KMC give back the same results.

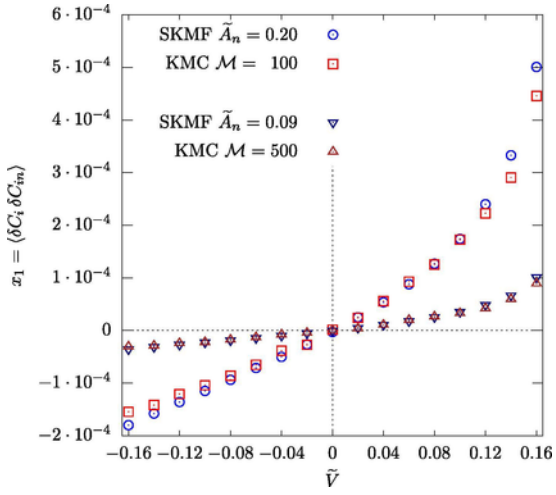


**Fig. 5.** The dependence of $x_1 \equiv \langle \delta C_i \delta C_{in} \rangle$ on $\widetilde{V}$ in SKMF and KMC. For visualization the $\widetilde{A}_n^2$ and $\mathscr{M}$ parameter pairs were chosen based on the similar $x_0$ dispersion values in the case of $\widetilde{V}=0$. (See Fig. 1.).

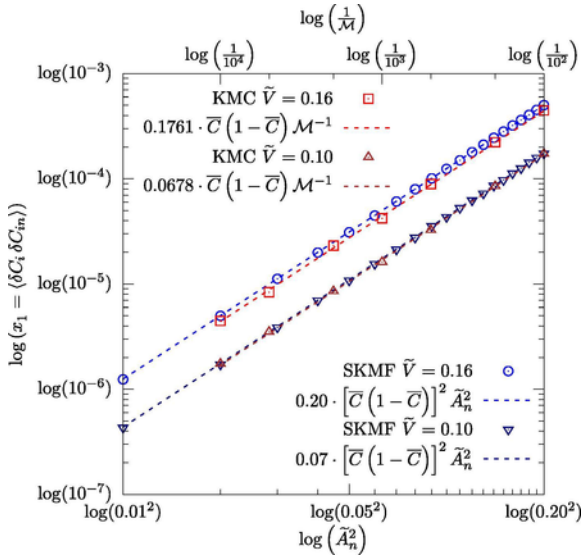


**Fig. 6.** Dependence of $x_1 \equiv \langle \delta C_i \delta C_{in} \rangle$ on $\widetilde{A}_n^2$ in SKMF and $\mathcal{M}^{-1}$ in KMC for two values of $\widetilde{V}$ and fitted functions based on Eqs. (28) and (29). Due to the double-logarithmic plotting the proportional connection is shown as a straight line with slope 1.

:

$$x_1^{\mathrm{SKMF}} = k_1^{\mathrm{SKMF}} \times \left[\overline{C}\left(1-\overline{C}\right)\widetilde{A}_n\right]^2, \tag{28}$$

$$x_1^{\mathrm{KMC}} = k_1^{\mathrm{KMC}} \times \left[\overline{C}\left(1-\overline{C}\right)\mathcal{M}^{-1}\right]. \tag{29}$$

In Fig. 7. we show the fitted $k_1$ constants of proportionality as functions of $\widetilde{V}$. The results resemble the theoretically expected behavior again [30]. In terms of deviation between SKMF and KMC a similar tendency can be seen as in Fig. 3. The expected value of $x_1 \equiv \langle \delta C_i \delta C_{in} \rangle$ correlation parameter clearly depends on the expected value of $x_0 \equiv \langle \delta C_i \delta C_i \rangle$ dispersion. Considering again, that both $x_1$ and $x_0$ are both proportional to $\widetilde{A}_n^2$ squared noise amplitude in SKMF and to $\mathcal{M}^{-1}$ reciprocal averaged number of states in KMC:

$$\text{in SKMF}: \quad \frac{x_1^{\mathrm{SKMF}}}{x_0^{\mathrm{SKMF}}} = \frac{k_1^{\mathrm{SKMF}} \times \left[\overline{C}\left(1-\overline{C}\right)\widetilde{A}_n\right]^2}{k_{0,\mathrm{site}}^{\mathrm{SKMF}} \times \left[\overline{C}\left(1-\overline{C}\right)\widetilde{A}_n\right]^2} = \frac{k_1^{\mathrm{SKMF}}}{k_{0,\mathrm{site}}^{\mathrm{SKMF}}}, \tag{30}$$

$$\text{in KMC}: \quad \frac{x_1^{\mathrm{KMC}}}{x_0^{\mathrm{KMC}}} = \frac{k_1^{\mathrm{KMC}} \times \left[\overline{C}\left(1-\overline{C}\right)\cdot\mathcal{M}^{-1}\right]}{k_{0,\mathrm{site}}^{\mathrm{KMC}} \times \left[\overline{C}\left(1-\overline{C}\right)\cdot\mathcal{M}^{-1}\right]} = \frac{k_1^{\mathrm{KMC}}}{k_{0,\mathrm{site}}^{\mathrm{KMC}}}, \tag{31}$$

$x_1/x_0 = k_1/k_{0,\mathrm{site}}$ is another measure, which should depend only on the thermodynamic parameters. This is exactly what we can see in Fig. 8, where the values of $k_1/k_0$ from SKMF and KMC are very close to each other. In Fig. 8 we show the results for two other average compositions ($\overline{C}=0.3$ and $\overline{C}=0.1$), for which we also performed the simulations and comparisons, though, with smaller statistical samples. The data points are still in close proximity to each other, signifying that the deduced relationships hold also for other compositions. This is expected as we did not use the specific value of the average composition in our considerations.

## 5. Conclusions

We Investigated the effects of introducing stochasticity into 3D atomistic kinetic mean-field simulations by studying of dispersion and correlations in equilibrium regular solutions by numeric simulations using SKMF method and atomistic kinetic Monte Carlo simulations. The results demonstrated that under the investigated, high temperature, equilibrium conditions the introduction of the noise of atomic flux into kinetic mean-field is equivalent to averaging over the finite number of copies within the canonical ensemble (or over the Monte Carlo runs).

Dispersion and correlation are proportional to the squared noise amplitude (inversely proportional to number of system copies).

Proportionality factor $k_{0,\mathrm{site}}$ for dispersion per one site is non-monotonic, since tendency to ordering as well as tendency to decomposition leads to larger oscillations at atomic scale.

Proportionality factor $k_{0,\mathrm{cluster}}$ for dispersion per cluster is monotonic, since tendency to oscillations from site to site at negative mixing energies is averaged and smeared even over the cluster of 13 sites.

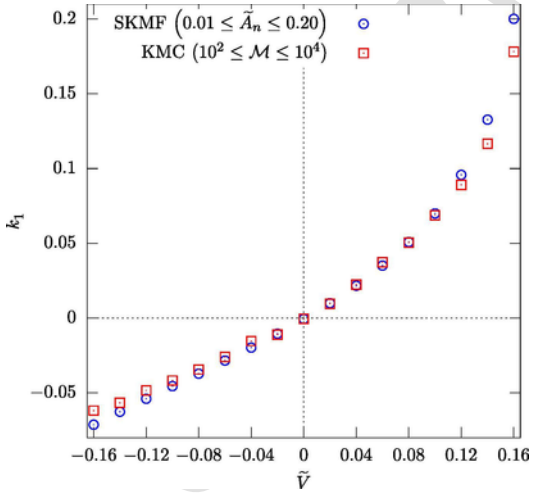


**Fig. 7.** Dependence of fitted proportionality factor $k_1$ on $\widetilde{V}$ in Eqs. (28) and (29). The relative asymptotic standard error of fitting $k_1$ to the average $x_1$ values remained under 0.5% for all cases of SKMF and under 3.0% for all cases of KMC (with the natural exceptions of the values at the origin.) Error bars are not shown for the sake of clarity as they would be similar in size to the markers used.

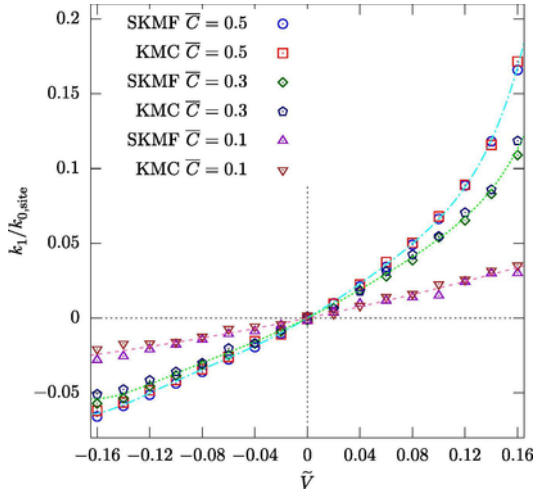


**Fig. 8.** Fitted constants of proportionality $k_1$ from Eqs. (28) and (29) (See Fig. 7.) divided by the according fitted constants of proportionality $k_{0,\mathrm{site}}$ from Eqs. (22) and (23) (See Fig. 2.). At a certain $\overline{C}$ average composition $k_1/k_{0,\mathrm{site}}$ depends only on the thermodynamic parameters of the system and accordingly, SKMF and KMC give back the same results. We show the match at three different average compositions. The dashed lines are just for guiding the eye.

Proportionality factor $k_1$ for correlation, is negative for negative mixing energy and positive for positive mixing energy.

SKMF method is applicable to simulation of homophase fluctuations and its statistical behavior in terms of fluctuation and spatial correlation can be perfectly matched with those of averaged Monte Carlo simulations following the relationship:

$$\mathcal{M} = \frac{\overline{\Gamma}}{\left[\overline{C}\left(1-\overline{C}\right)A_n^2\right]}.$$

The natural next step should be to test if these properties are transferred to heterogeneous fluctuations at lower temperatures leading to nucleation. Due to the complex nature of that problem it will be investigated in another paper. Based on the results of this work the authors expect that for keeping the analogy between the two techniques at least the averaging scheme for kinetic Monte Carlo should be modified for the preservation of time-correlations.

## Author contributions statement

A.M.G. and Z.E. conceived the project. T.V.Z. wrote an independent version of SKMF code, acquired the simulation results and processed the data for the case of $\overline{C} = 0.5$. A.T. modified Z.E.'s kinetic Monte Carlo code for purpose and wrote the software to analyze the data. G.J. modified the original SKMF code for purpose and analyzed the data for $\overline{C} \neq 0.5$ cases and checked the results with an independent code for the $\overline{C} = 0.5$ case. A.M.G. was responsible the theoretical derivations and descriptions, while T.V.Z. checked the theoretical results. A.M.G and J.J.T. wrote the manuscript. J.J.T. prepared the figures, checked the theoretical results, formatted and finalized the manuscript.

## Data availability statement

The SKMF software code to produce new sets of SKMF raw data can be downloaded from [32]. In present work we provided all the necessary input parameters to reproduce the results with the published code.
CRediT authorship contribution statement
**Tetyana V. Zaporozhets:** Data curation, Formal analysis, Investigation, Software, Validation. **Andriy Taranovskyy:** Data curation, Investigation, Software. **Gabriella Jáger:** Data curation, Investigation, Software, Validation. **Andriy M. Gusak:** Conceptualization, Funding acquisition, Formal analysis, Project administration, Supervision, Writing - original draft. **Zoltán Erdélyi:** Conceptualization, Funding acquisition, Project administration, Resources, Software, Supervision. **János J. Tomán:** Investigation, Formal analysis, Project administration, Software, Supervision, Visualization, Writing - review & editing.

## Acknowledgments

This work was supported in part by Ministry of Education and Science of Ukraine (project 0118U003861), by EXMONAN EU FP7 project (Ref. 612552) and by GINOP-2.3.2-15-2016-00041 project co-financed by the European Union and the European Regional Development Fund.

## Appendix A. Supplementary data

Supplementary data associated with this article can be found, in the online version, athttps://doi.org/10.1016/j.commatsci.2019.109251.

## References

[1] J.D. van der Waals, The thermodynamic theory of capillarity under the hypothesis of a continuous variation of density, J. Stat. Phys. 20 (2) (1979) 200–244.
[2] A.A. Vlasov, Many-particle theory and its application to plasma. Translated from the Russian. Gordon and Breach Science Publishers Inc, New York.
[3] Власов А.А. Нелокальная статистическая механика, URSS, 2011.
[4] P. Anderson, Generalizations of the Weiss molecular field theory of antiferromagnetism, Phys. Rev. 79 (4) (1950) 705.
[5] P.-O. Löwdin, Quantum theory of many-particle systems. ii. study of the ordinary hartree-fock approximation, Phys. Rev. 97 (6) (1955) 1490.
[6] R.H. Fowler, E.A. Guggenheim, Statistical thermodynamics of super-lattices, Proc. R. Soc. Lond. A 174 (957) (1940) 189–206.
[7] A. Khachaturyan, Theory of structural transformations in solids, John Wiley & Sons, New York.
[8] G. Martin, Atomic mobility in Cahn's diffusion model, Phys. Rev. B 41 (4) (1990) 2279.
[9] Z. Erdélyi, I.A. Szabó, D.L. Beke, Interface sharpening instead of broadening by diffusion in ideal binary alloys, Phys. Rev. Lett. 89 (16) (2002), 165901.
[10] Z. Erdélyi, M. Sladecek, L.-M. Stadler, I. Zizak, G.A. Langer, M. Kis-Varga, D.L. Beke, B. Sepiol, Transient interface sharpening in miscible alloys, Science 306 (5703) (2004) 1913–1915.
[11] C. Cserháti, H. Bakker, D. Beke, Kinetics of surface segregation in alloys, Surf. Sci. 290 (3) (1993) 345–361.
[12] C. Cserháti, I.A. Szabó, D.L. Beke, Size effects in surface segregation, J. Appl. Phys. 83 (6) (1998) 3021–3027.
[13] A. Gusak, T. Zaporozhets, Martin's kinetic mean-field model revisited-frequency noise approach versus monte carlo, Metallofiz. Noveishie Tekhnol. 40 (11) (2018) 1415–1435, https://doi.org/10.15407/mfint.40.11.1415, arXiv: https://doi.org/10.15407/mfint.40.11.1415.
[14] Y. Wang, L.-Q. Chen, A. Khachaturyan, Computer simulation of microstructure evolution in coherent solids, PTM'94, Solid-to-Solid Phase Transf. (1994) 245–265.
[15] Y. Wang, D. Banerjee, C. Su, A. Khachaturyan, Field kinetic model and computer simulation of precipitation of l12 ordered intermetallics from f.c.c. solid solution, Acta Mater. 46 (9) (1998) 2983–3001.
[16] D.L. Beke, Z. Erdélyi, Resolution of the diffusional paradox predicting infinitely fast kinetics on the nanoscale, Phys. Rev. B 73 (2006)035426https://doi.org/10.1103/PhysRevB.73.035426, URL: https://link.aps.org/doi/10.1103/PhysRevB.73.035426.
[17] D.L. Beke, Atomic interpretation of the interface transfer coefficients for interdiffusion in ab binary phase separating system, Int. J. Heat Mass Transf. 113 (2017) 203–209, https://doi.org/10.1016/j.ijheatmasstransfer.2017.05.074, URL: http://www.sciencedirect.com/science/article/pii/S0017931017313789.
[18] N.V. Storozhuk, K.V. Sopiga, A.M. Gusak, Mean-field and quasi-phase-field models of nucleation and phase competition in reactive diffusion, Philos. Mag. 93 (16) (2013) 1999–2012.
[19] D.L. Beke, C. Cserháti, Z. Erdélyi, I.A. Szabó, Segregation in nanostructures, in: H. Nalwa (Ed.), Nanoclusters and Nanocrystals, Nanotechnology book series, American Scientific Publishers, 2003, Ch. 7.
[20] Z. Erdélyi, M. Pasichnyy, V. Bezpalchuk, J.J. Tomán, B. Gajdics, A.M. Gusak, Stochastic kinetic mean field model, Comput. Phys. Commun. 204 (2016) 31–37.
[21] A. Gusak, T. Zaporozhets, N. Storozhuk, Phase competition in solid-state reactive diffusion revisited-stochastic kinetic mean-field approach, J. Chem. Phys. 150 (17) (2019) 174109, https://doi.org/10.1063/1.5086046, arXiv: https://doi.org/10.1063/1.5086046.
[22] G.E.P. Box, M.E. Muller, A note on the generation of random normal deviates, Ann. Math. Statist. 29 (2) (1958) 610–611, https://doi.org/10.1214/aoms/1177706645.
[23] V.M. Bezpalchuk, M.O. Pasichnyy, A.M. Gusak, Application of a stochastic kinetic mean field (SKMF) method to ordering substitutional atoms in macro-and nanosize fcc lattices, Metallofiz. Noveishie Tekhnol. 38 (2016) 1135–1144.
[24] B.D. Gajdics, J.J. Tomán, F. Misják, G. Radnóczi, Z. Erdélyi, Spinodal decomposition in nanoparticles – experiments and simulation, In: Diffusion in Materials DIMAT-2017, Vol. 383 of Defect and Diffusion Forum, Trans Tech Publications, 2018, pp. 89–95.
[25] V.M. Bezpalchuk, R. Kozubski, A.M. Gusak, Simulation of the tracer diffusion, bulk ordering, and surface reordering in fcc structures by kinetic mean-field method, Uspekhi Fiziki Metallov-Prog. Phys. Metals 18 (3) (2017) 205–233.
[26] V.M. Bezpalchuk, D.S. Rusenko, A.M. Gusak, Influence of the intermediate nanointerlayer on a kinetics of phase formation and ordering in thin films-mean-field kinetic simulation (in ukrainian), Metallofiz. Noveishie Tekhnol. 39 (2017) 865–879.
[27] L. Landau, E. Lifshitz, M. Kearsley, L. Pitaevskii, J. Sykes, Statistical Physics, In: no. pt. 1 in Course of Theoretical Physics, Elsevier Science, 1996.
[28] S.W. Roberts, Control chart tests based on geometric moving averages, Technometrics 1 (3) (1959) 239–250, https://doi.org/10.1080/00401706.1959.10489860, arXiv: https://amstat.tandfonline.com/doi/pdf/10.1080/00401706.1959.10489860.
[29] D. Montgomery, Introduction to Statistical Quality Control, Wiley, 2009, URL:https://books.google.hu/books?id=oG1xPgAACAAJ.
[30] T.V. Zaporozhets, A. Taranovskyy, G. Jáger, A.M. Gusak, Z. Erdélyi, J.J. Tomán, Supplementary materials for, the effect of introducing stochasticity to kinetic mean-field calculations: comparison with lattice kinetic monte carlo in case of regular solid solutions', Comput. Mater. Sci.
[31] W. Press, J. Wevers, B. Flannery, C.U. Press, S. Teukolsky, W. Vetterling, N.R. Software, W. Vetterling, B. Flannery, Numerical Recipes in C: The Art of Scientific Computing, In: v. 1 in Numerical Recipes in C book set, Cambridge University Press, 1992, URL: https://books.google.hu/books?id=DvCHStDs_I4C.
[32] Official Stochastic Kinetic Mean Field website (Accessed: 2018–10-15). URL:http://skmf.eu.